Modeling of Ir adatoms on Ir surfaces

C. M. Chang and C. M. Wei
Institute of Physics, Academia Sinica, Nankang, Taipei, 11529 Taiwan, Republic of China

S. P. Chen
Theoretical Division, Los Alamos National Laboratory, Los Alamos, New Mexico 87545

(Received 30 August 1996)

We used the embedded-atom method potential to study the structures, adsorption energies, binding energies, migration paths, and energy barriers of the Ir adatom and small clusters on fcc Ir (100), (110), and (111) surfaces. We found that the barrier for single-adatom diffusion is lowest on the (111) surface, higher on the (110) surface, and highest on the (100) surface. The exchange mechanisms of adatom diffusion on (100) and (110) surfaces are energetically favored. On all three Ir surfaces, Ir_2 dimers with nearest-neighbor spacing are the most stable. On the (110) surface, the Ir_2 dimer diffuses collectively along the $\langle 110 \rangle$ channel, while motion perpendicular to the channel walls is achieved by successive one-atom and correlated jumps. On (111) surface, the Ir_2 dimer diffuses in a zigzag motion on hcp and fcc sites without breaking into two single atoms. On the (100) surface, diffusion of the Ir_2 dimer is achieved by successive one-atom exchange with the substrate atom accompanying by a 90° rotation of the Ir_2 dimer. This mechanism has a surprisingly low activation energy of 0.65 eV, which is 0.14 eV lower than the energy for single adatom exchange on the (100) surface. Trimers were found to have a one-dimensional (1D) structure on (100) and (110) surfaces, and a 2D structure on the (111) surface. The observed abrupt drop of the diffusion barrier of tetramer, I_{γ_4} on the Ir (111) surface was confirmed theoretically. [S0163-1829(96)06647-7]

I. INTRODUCTION

A fundamental element of many surface phenomena, nucleation and growth of crystals is adatom behavior on solid surfaces.[1] These atomic processes include surface diffusion of single adatom and small clusters, interaction of adatoms with the substrate, association of atoms into clusters, dissociation of clusters, etc. The structures and diffusion mechanisms of adatom clusters have been studied extensively by field ion microscopy (FIM).[2,3] Although FIM is limited to only a handful of metal surfaces: platinum,[4,5] rhodium,[3] nickel,[6] tungsten,[7–11] iridium,[12–20] tantalum,[21] molybedenum,[22] and aluminum,[23] which can sustain the high field used for imaging, it does provide detailed real-space images of the atom clusters, quantitative energies of the site binding, and diffusion barriers. These systems were also the subject of several theoretical studies.[24–38] The Ir surfaces are the most studied system experimentally, but to our knowledge no theoretical studies exist at the moment. Here we present an extensive theoretical study of the detailed structures and diffusion behaviors of Ir adatoms on many Ir surfaces.

In terms of theoretical studies of adatoms on surfaces, the choice of a reliable potential for a given metallic system is essential. The traditional approach has been to use pairwise potentials such as the well-known Morse potential and Lennard-Jones potential because of their computational simplicity. These types of pairwise potentials have been used successfully to treat inert impurities, such as He in metals,[39] but the method is not applicable to chemically active impurities[39,40] owing to the many-body effects of electronic origin. There are two important failures of two-body interactions: the unrelaxed vacancy formation energy is the same as the cohesive energy, and the Cauchy pressure $(C_{12}-C_{44})$ is zero. Neither of these conditions holds in real solids. These problems can be remedied by introducing a many-body term in addition to a pairwise potential. Daw and Baskes developed an embedded-atom method (EAM) (Refs. 40–44) potential which separates the energy of the system into a pairwise term plus an ''embedding'' term for each atom. The embedding term is a function of the local electron density that an atom senses due to its nearby atoms. This additional embedding term makes it possible to treat chemically active as well as inert impurities in one unified theory. In essence, the embedding energy provides a local ''volume'' or ''density'' term for each atom, so that large variations in local density can be described accurately. The EAM has demonstrated the ability to describe fcc transition metals with filled or nearly filled *d* bands accurately (especially Ni and Cu column elements). Some deficiencies in treating bcc metals were noted.[36] Simulation results using these potentials show dramatic improvement over pairwise potentials,[22,32–35,43–57] with only twice the computational effort.

Recently, some interesting results were obtained regarding self-diffusion and adatom diffusion on Ir surfaces as well as other fcc metals[22,32–35,44–48] bcc metals,[36,49] and hcp metals.[50] The Voter-Chen formalism for fitting the EAM potentials[44–46] was applied successfully to studies of fcc, bcc, and hcp metals with or without impurities.[46–50] We used the same style potential for Ir (Ref. 48) to study Ir clusters and their diffusions on Ir surfaces, because many FIM results are available to compare with the results. In particular, we restrict our attention on structures and surface diffusions of adatoms, since these phenomena involve many basic and important mechanisms. We will summarize previous experimental and theoretical results in Sec. II. The relevant details

of the EAM are outlined in Sec. III. The calculated results and comparisons with experiments are presented in Sec. IV. Conclusions are presented in Sec. V.

II. SUMMARY OF PREVIOUS EXPERIMENTAL AND THEORETICAL RESULTS

It has been proposed and shown that adatoms on fcc(111) surface diffuse faster than on either (110) or (100) surfaces.[12–20,24–27,57] Based on the hard-sphere model of the surface, an adatom is expected to jump along the surface direction of the least corrugation. In fact, most experimental data are consistent with this assumption, except when atomic exchange occurs. As far as we know, there are two exceptions. First, on the fcc(100) surface of some metals, surface diffusion may occur by an exchange mechanism. Second, on the (110) surface of some fcc metals, an adatom can jump either along the surface channel direction or through the surface channel by the exchange mechanism. The adatom tends to hop on (100) and (110) surfaces of Ni (Ref. 6) and Rh,[3] and on the (111) surface for most fcc metals, but it exchanges on Ir (Refs. 12 and 17–19) and Pt (Refs. 5 and 30) (110) and (100) surfaces. Feibelman[29] and Liu *et al.*[25] showed theoretically that Al, Pt, and Au might have an exchange mechanism on a (100) surface but not for other fcc metals. Roelofs and Martir[58] also concluded that, on the Au(110) surface, the exchange mechanism needs less energy than is required to hop cross channel. An effective-medium theory calculation gives a similar conclusion for diffusion of an Al adatom on Al(100) and (110) surfaces.[59] Many researchers observed the diffusion motion by cross-channel exchange on Ir(110),[12,18,19] and on the Ir(100) surface.[17,18] For Ir_2 dimers, FIM experiments showed that Ir_2 dimers on the Ir(110) surface can diffuse across surface channels as well as along these channels.[20] On the (111) surface, Ir_2 dimer diffusion between fcc sites and hcp sites was also reported.[15] To our knowledge, no experimental results exist for Ir_2 dimers on the Ir(100) surface.

FIM studies of Ir clusters[14–19] on Ir (111), (110), and (100) surfaces indicate that the favored trimers or N-mers (with N greater than 2) configurations may be one-dimensional (1D) (linear) or two-dimensional (2D) structures. For example, the 1D structure of the Ir trimer is more stable on the Ir(100) surface, while the 2D structure of the Ir trimer is more stable on the Ir(111) surface. The repulsions of two adatoms at a second-nearest-neighbor distance have also been proposed to explain the 1D structure and the (1×5) reconstruction of the Ir(100) surface at high temperature.[12] For small clusters on the Ir(111) surface, FIM experiments found that the activation energy increases sharply from the single adatom to the dimer and from the dimer to the trimer, drops for the tetramer, and then rises again.[15] Dimers and other N-mers may diffuse together or individually. To our knowledge, no theoretical results exist for Ir. We have used an Ir EAM potential to study Ir adatoms on many Ir surfaces, and check our results against available FIM results.

III. COMPUTATIONAL METHOD

Embedded-atom methods[44–50] are based on density-functional theory, in which the electron density uniquely specifies the potential, and thus the energy is a functional of the density. Since each atom can be viewed as an impurity embedded in a host comprising all the other atoms, and the energy of an impurity is a functional of the electron density of the host, thus the total energy of an N-particle system is written as

$$E_{\rm tot}=\tfrac{1}{2}\sum_{i}^{n}\sum_{j\neq i}^{n}\phi(r_{ij})+\sum_{i}^{n}F[\rho_i]. \tag{1}$$

Here r_{ij} is the scalar distance between atoms i and j, ϕ is a pairwise potential which accounts for the classical electrostatic interaction, and ρ_i is the density at atomic site i due to all its neighbors,

$$\rho_i=\sum_{j\neq i}^{n}\rho(r_{ij}). \tag{2}$$

The embedding energy $F[\rho_i]$ can be interpreted as the energy arising from embedding atom i in an electron gas of density ρ_i. In the Voter-Chen formalism,[44] the pairwise term $\phi(r)$ is taken to be a Morse potential,

$$\phi(r)=D_M\{1-\exp[-\alpha_M(r-R_M)]\}^2-D_M. \tag{3}$$

The three parameters D_M, R_M, and α_M define the depth, the distance to the minimum, and a measure of the curvature near the minimum, respectively. The density function $\rho(r)$ is taken as

$$\rho(r)=r^6[e^{-\beta r}+512e^{-2\beta r}], \tag{4}$$

where β is an adjustable parameter. These adjustable parameters are specified in the fitting procedure, and their values will be given below. The embedding functional $F[\rho]$ is specified by requiring that the energy of the fcc crystal behaves properly as the lattice constant is varied.[44] Rose *et al.*[60] showed that the cohesive energy of most metals can be scaled to a simple universal function, which is approximately

$$E_U(a^*)=-E_0(1+a^*)e^{-a^*}, \tag{5}$$

where a^* is a reduced distance variable, and E_0 is the depth of the function at the minimum ($a^*=0$). The appropriate scaling is obtained by taking E_0 as the equilibrium cohesive energy of the solid ($E_{\rm coh}$), and defining a^* by

$$a^*=\frac{\left(\dfrac{a}{a_e}-1\right)}{\left(\dfrac{E_{\rm coh}}{9B\Omega}\right)^{1/2}}, \tag{6}$$

where a is the lattice constant, a_e is the equilibrium lattice constant, B is the bulk modulus, and Ω is the equilibrium atomic volume. Thus, knowing $E_{\rm coh}$, a_e, and B, the embedding function is defined by requiring that the crystal energy from Eq. (1) match the energy from Eq. (5) for all values of a^*. By fitting $F[\rho]$ in this way, the potential should behave properly over a wide range of densities.

To be suitable for use in atomistic simulations, the interatomic potential, and its first derivatives with respect to nuclear coordinates, should be continuous at all geometries

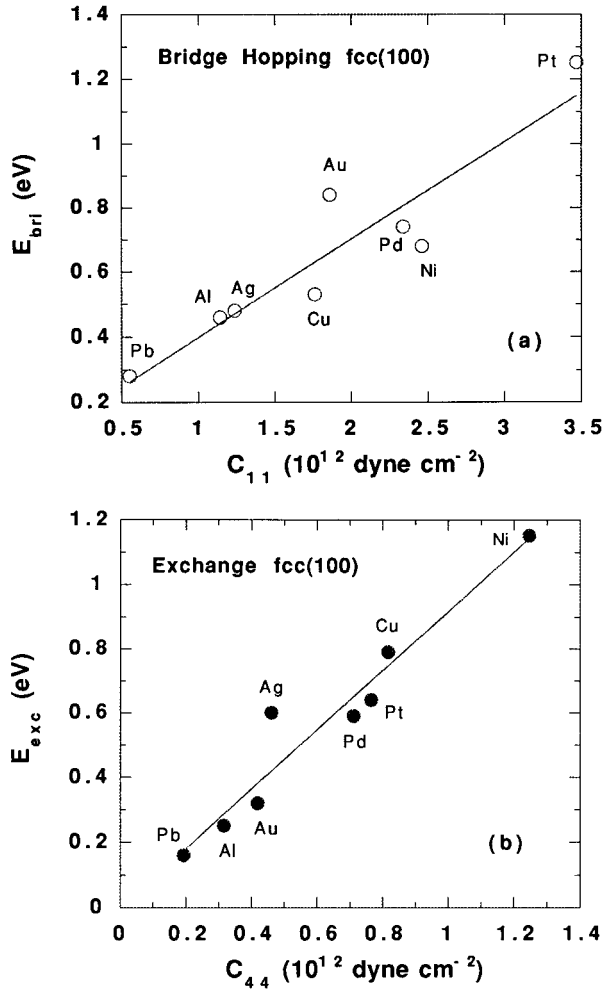

FIG. 1. The relation between the elastic constant C_{ij} and the self-diffusion barrier on the fcc(100) face. (a) The relation of C_{11} and the energy barrier over the ⟨111⟩ bridge. (b) The relation of C_{44} and the diffusion barrier along the ⟨112⟩ direction (exchange mechanism).

of the system. This is accomplished by forcing $\phi(r)$, $\phi'(r)$, $\rho(r)$, and $\rho'(r)$ to go smoothly to zero at $r=r_{\rm cut}$ by defining

$$f_{\rm smooth}(r)=f(r)-f(r_{\rm cut})+\left(\frac{r_{\rm cut}}{m}\right)\left[1-\left(\frac{r}{r_{\rm cut}}\right)^m\right]\left(\frac{df}{dr}\right)_{r=r_{\rm cut}}, \tag{7}$$

where $f(r)$ denotes $\phi(r)$ or $\rho(r)$ and $m=20$, with $r_{\rm cut}$ optimized in the fitting procedure. After the potential has been determined, the force on the ith atom F_i is obtained from the derivatives of the potential [Eq. (1)]. In the energy minimization mode, the atoms were moved in the direction of the force by an amount proportional to the force. This is repeated until the maximum force is less than a specified tolerance limit (10^{-3} eV/Å in this case).

fcc(100) surface diffusion barriers through an exchange mechanism along ⟨112⟩ are roughly linearly related to C_{44} for many fcc metals (Ni, Cu, Al, Ag, Au, Pd, Pt, and Pb), while the barriers over the bridge site along ⟨111⟩ are also linearly related to C_{11}, as shown in Fig. 1. The calculated results are taken from present calculation and Ref. 25. This type of correlation to elastic constants is easily imagined in the dynamical theory of atom diffusions, as discussed in Ref. 61. This correlation indicates that only certain normal modes of shear motions related to C_{44} are relevant to the exchange mechanism of fcc(100) surface diffusion. This correlation of small C_{44} to a small diffusion barrier also seems to fit with the observation that fcc metals, which reconstruct on (110), tend to favor the exchange mechanism for adatom diffusions.[14,62] In this paper, we modified the original Ir potential, which is successful in treating surface reconstruction and grain boundary fracture problems but gives an unrealistically high energy for the Ir exchange diffusion barrier (2.80 eV) on the (100) surface,[48] to fit the diffusion barrier of the (100) self-diffusion barrier of 0.84 eV. In doing this we have allowed the elastic constant of C_{ij} fluctuate to satisfy the fit to the diffusion energy. The resulting surface Ir potential is suitable for describing the surface diffusion and reconstructions. The resulting calculated (experimented) lattice constant is 3.84 (3.84) Å, the cohesive energy is 6.94 (6.94) eV/atom, the bulk modulus is 3.70 (3.70), C_{11} is 4.245 (5.995), C_{12} is 3.428 (2.558), and C_{44} is 1.054 (2.688)$\times 10^{12}$ dyn/cm^2. The parameters of the Ir surface potential are as follows: $D_M=0.777\ 939$ eV, $R_M=2.520\ 03$ Å, $\alpha_M=2.169\ 85$ Å^{-1}, $\beta=3.899\ 27$ Å^{-1}, and $r_{\rm cut}=5.3548$ Å. The 1×2(110) surface energy is lower than the 1×1 surface energy of 1897 mJ/m^2 by 86 mJ/m^2, which is consistent with observed 1×2 reconstructions on the Ir(110) surface. The surface phonons are ~30% (~20%) softer than the original Ir potential (experiment), but we must compromise to obtain reasonable diffusion energies. This Ir surface potential is therefore capable of describing the surface reconstruction and diffusion on the Ir surface reasonably well, as demonstrated here and in the results described below. The calculations are done on at least $4a_e$ by $4a_e$ cell sizes, with free surfaces in the z direction and periodic boundary conditions in the x and y directions.

IV. RESULTS AND DISCUSSION

In this section, we report the simulation results in two major parts: cluster structures in Sec. IV A and surface diffusion in Sec. IV B. The adsorption sites and adsorption energies of single adatoms on Ir(100), (110), and (111) surfaces are discussed in Sec. IV A 1. Section IV A 2 describes the stable Ir_2 structures and binding energies on all three faces. The stable 1D or 2D configurations for trimers are reported in Sec. IV A 3. The diffusion mechanisms and activation energies of single adatoms and dimers on all three surfaces are given in Secs. IV B 1 and IV B 2, respectively. The diffusion barriers of small clusters containing up to five adatoms on the Ir(111) surface are discussed in Sec. IV B 3.

The surface relaxation plays an important role in the atomic exchange diffusion mechanisms, but not so important a role for the hopping mechanisms. For example, the energy barriers of a single adatom diffusing on a (100) surface with (without) surface relaxation are 0.79 (2.46) eV (atomic exchange), 1.58 (1.61) eV (hop across bridge site) and 2.66 (2.83) eV (hop over atop site). The energies discuss in the following sections are all full-relaxation cases.

A. Structure and stability

1. Single adatom

To find the adsorption site and adsorption energy of a single adatom on surfaces in the simulations, we put an ada-

TABLE I. Adsorption energies E_{ad} of an Ir single adatom on Ir surfaces.

Surface	Calculation (eV)	Experiment (eV)
(100)	5.89	6.38±0.20 (Ref. 17)
(110)	6.49	
(111)	4.95	

tom above the top surface layer with a spacing less than r_{cut} (5.3548 Å), then allow the whole system to relax to the minimum-energy geometry (with maximum forces on any atom less than 10^{-3} eV/Å). The adsorption energy E_{ad} is defined as the energy difference between the state of an adatom sitting at the adsorption site and the state of an adatom above the surface with a distance larger than r_{cut}.

On the Ir(100) surface, the Ir adatom most likely sits at the fourfold hollow site, and has four nearest neighbors on the top layer. For the Ir(110) surface, the Ir adatom generally sits at the surface channel site. At this site, the adatom has four nearest neighbors on the channel walls, and one nearest neighbor right below the channel. The situation on the Ir(111) surface is more complicated. There are two distinct sites, namely, the hcp site (surface site) and fcc site (bulk site). Wang and Ehrlich[15] suggested that the hcp site is more stable than the fcc site, with an energy difference of 0.016 eV. Both the fcc and hcp sites have three nearest neighbors on the surface layer. In our calculations, the energy difference is extremely small (0.0001 eV); therefore, we expect that the Ir adatom has only a slight preference for sitting at a hcp site on the (111) face in our potential model.

The calculated results of adsorption energies of the adatom on Ir surfaces are listed in Table I. The adsorption energy is the lowest (4.95 eV) on the Ir(111) surface, higher (5.89 eV) on the (100) surface, and the highest (6.49 eV) on the (110) surface. All these energies are lower than the bulk cohesive energy of 6.94 eV.[48] The binding energy on the (100) surface of 5.89 eV is slightly lower than the value inferred from the FIM results of 6.38±0.20 eV.[17] The relative magnitudes of the binding energies on these surfaces may be understood easily from the environment of the adsorbed site, as discussed above. On the close-packed (111) surface, the adsorbed adatom formed only three bonds with the top surface layer atoms, while on the loosely packed (100) surface there are four bonds between the adatom and the top layer surface atoms, and on the channeled (110) surface there are five nearest-neighbor bonds (four with the top layer atoms and one with the second layer atom right below the adatom). These bond counting trends are consistent with our calculations of the adsorption energies.

2. Dimers

For Ir dimers, we focus our attention on the equilibrium energies of total system with two adatoms sitting at nearest, second-nearest, and the third-nearest-neighbor distances (see Fig. 2). When two adatoms sit at the third-nearest-neighbor distance, the distance between these two adatoms is 5.44 A, which is slightly larger than the value r_{cut}=5.3845 A used in the calculation. We found that the interaction between these two adatoms is very weak, and these two atoms can be viewed as nearly isolated. Therefore, we can approximate the energy difference between two adatoms sitting at nearest-neighbor and third-nearest-neighbor distances as binding energies of the dimer, E_b. The energy difference between the second-nearest and third-nearest neighbors are also calculated. The calculated results of the binding energies and the dimer length of Ir_2 on Ir surfaces are given in Table II.

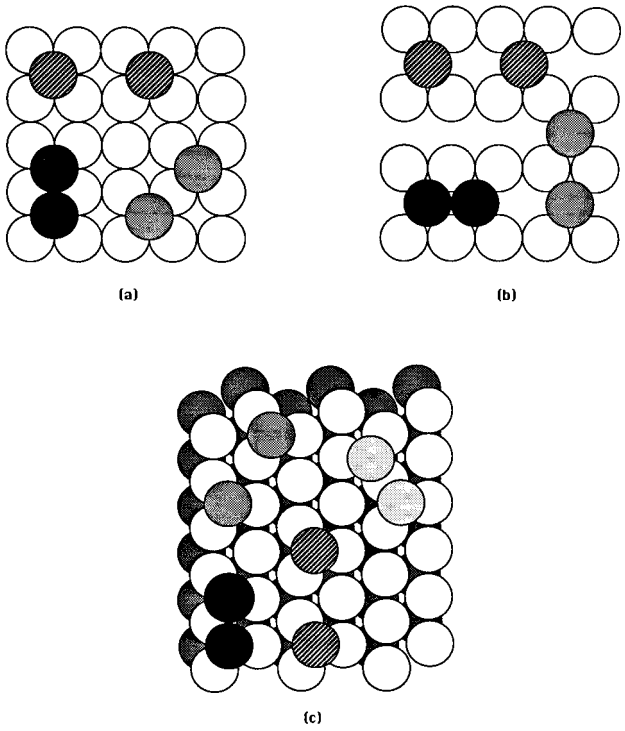

FIG. 2. Two adatoms sit with various distances on various surfaces. The nearest neighbors (black circles), second-nearest neighbors (gray circles), and third-nearest neighbors (dashed circles) for the (100) surface (a), the (110) surface (b), and the (111) surface (c). The light gray circles of (c) show the forbidden state for two adatoms, with one at the fcc site and the other one at the hcp site.

From these results we found that, on all three Ir surfaces, Ir_2 dimers with the nearest-neighbor distance are the most stable. Similar to a single adatom on the Ir(111) surface, the Ir_2 dimer also has two adsorption sites: hcp and fcc sites. In the calculation, the energy difference of these two types of sites is again very small, and the dimer might sit either on a hcp or fcc site. It is interesting to note that the difference is unfavorable (+0.17 eV) when the two adatoms are at second-nearest-neighbor distance occupying sites of different types (i.e., one at a fcc site and the other at a hcp site), as illustrated in Fig. 2. Thus we conclude that the Ir_2 dimer must remain at the same kind of sites, i.e., both on hcp sites or on fcc sites at the same time. This understanding is very helpful in studying the diffusion mechanism of an Ir_2 dimer on the Ir(111) surface, which we will discuss below.

The dimer binding energies of Ir_2 at the nearest-neighbor distance are 0.79, 0.64, and 1.10 eV, corresponding to (100), (110), and (111) surfaces, respectively. These calculations show that dimers are stable on all three surfaces which are consistent with the experiments.[14,15] Agreement within a factor of 2 was obtained for an Ir(110) surface of 1.10±0.11 eV.[17] The binding energy is highest on the Ir(111) surface,

TABLE II. Binding energies and dimer length of Ir dimers on Ir surfaces.

Surface	Binding length	Calculated binding energies (eV)	Experimental binding energies (eV)
(100)	nearest neighbor 2.72 Å	0.79	
	second nearest neighbor 3.84 Å	−0.03	
	third nearest neighbor 5.44 Å	0.0	
(110)	nearest neighbor 2.72 Å	0.64	1.10±0.11 (Ref. 17)
	second nearest neighbor 3.84 Å	−0.03	
	third nearest neighbor 5.44 Å	0.0	
(111)	nearest neighbor 2.72 Å	1.10	
	second nearest neighbor 4.72 Å	0.02	
	third nearest neighbor 5.44 Å	0.0	

lower on the Ir(100) surface, and the lowest on the Ir(110) surface. Because the binding energy in the EAM comes from the embedding energy, which depends on the local electron density,[32] these results are reasonable since the (111) surface is the most densely packed, the (110) surface is less densely packed, and the (100) surface is the most loosely packed. We also found that, on the (100) and (110) surfaces, the third-nearest-neighbor configurations are more stable than the second-nearest-neighbor configurations (Table II); this is due to the net repulsive interactions between the two adatoms sitting at the second-nearest-neighbor distance (due to the interactions of strain fields of adatoms). This repulsion, which has been confirmed in our calculation, at the second-nearest-neighbor distance for (100) and (110) surfaces has been proposed to explain the FIM results of a 1D structure in trimers.[15]

3. Trimers

A small cluster with three or more atoms might have either a one- or two-dimensional structure. Since three-atom clusters (trimers) are the smallest clusters which can still have 1D or 2D structure, here we report a study of structures of Ir trimers on all three Ir surfaces. For trimers, the structure may have a linear form or a triangular form, as shown in Fig. 3 for all three surfaces. We have found that trimers on both (100) and (110) surfaces are energy favored in 1D linear forms, while a 2D close-packed triangular form is favored on the (111) surface, which are in agreement with FIM results.[15] The energy differences between 1D and 2D structures, ΔE_{1D-2D}, are found to be 0.64, 0.04, and −0.95 eV for (110), (100), and (111) surfaces, respectively. The corresponding experimental energies for (100) and (111) are 0.348 eV and −0.098, respectively. The magnitudes of these experimental energies are not in good agreement, but the signs are consistent with our present calculations. Unfortunately, no experimental results for (110) exist. The cause of the stable 1D structures on (100) and (110) surfaces and the 2D structure on the (111) surface can be explained by repulsions at the second-nearest neighbors, which was reported in Sec. IV A 2. From Fig. 3, it is easily seen that, on the Ir(111) surface, the three atoms of 2D structure trimers all sit at the nearest-neighbor distance from each other, and form three nearest-neighbor bonds; however, for a linear trimer there

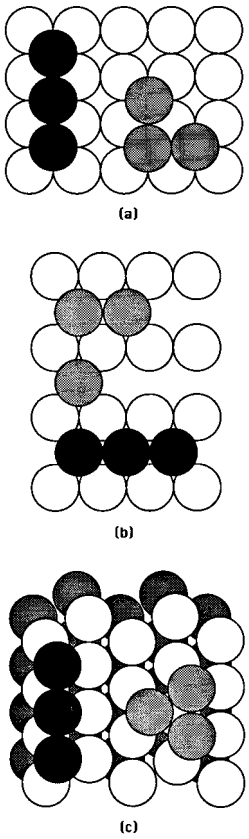

FIG. 3. 1D and 2D structures on three surfaces: (a) for (100), (b) for (110), and (c) for (111) surfaces.

TABLE III. Diffusion path and barriers of an Ir single adatom on Ir surfaces.

Surface	Diffusion path	Calculated E_m (eV)	Experimental E_m (eV)
(100)	hopping over atop site	2.66	---
	hopping across bridge site	1.58	>1.02 (Ref. 17)
	exchange	0.79	0.84±0.05 (Ref. 17)
(110)	hopping over atop site	3.65	
	hopping across bridge site	2.50	
	cross-channel exchange	0.81	0.71±0.02 (Ref. 17) 0.74 (Ref. 14)
	hopping along channel	0.70	0.80±0.04 (Ref. 17)
(111)	hopping over atop site	1.43	
	hopping across bridge site	0.11	0.22±0.04 (Ref. 17) 0.27±0.004 (Ref. 15)

are only two nearest-neighbor bonds, so the 2D structure is more stable on the (111) surface. For (100) and (110) surfaces, both the 1D and 2D structures have two nearest-neighbor bonds, but the 2D trimers on both surfaces have one additional repulsive bond, and cause the 1D structures to be more favorable than the 2D structures.

B. Surface diffusion

1. Single adatom

In this subsection, we report our study of self-diffusion of iridium adatoms on iridium (100), (110), and (111) surfaces. The energy barrier in the diffusion process is calculated according to

$$E_m = E_s - E_a , \tag{8}$$

where E_m is the barrier height which needs to be overcome for the self-diffusion, i.e., the migration energy; E_s is the energy with the adatom located at the saddle point along the diffusion path; and E_a is the energy with the adatom located at the adsorbed lattice site. The calculated results for migration energies and diffusion characteristics for various planes of the iridium are summarized in Table III. We found that the diffusion barrier for an Ir adatom on Ir(111) with the mechanism of hopping across a bridge site (the black circle of Fig. 4) is 0.11 eV, which is in fair agreement with FIM result of 0.27±0.004 (Ref. 15) and 0.22±0.04 eV.[17] The barrier for the unfavorable mechanism of hopping over an atop site (the gray circle of Fig. 4) is 1.43 eV, which is consistent with the fact that this mechanism was not observed in experiments.

On the Ir(110) surface, we found that the barrier height of diffusion along the ⟨110⟩ channel due to the hopping mechanism [the black circle of Fig. 5(b)] is 0.70 eV, while the exchange mechanism along the ⟨112⟩ or ⟨001⟩ directions (Fig. 6) has the same energy barrier of 0.81 eV. The experimental results are 0.80±0.04 and 0.71±0.02 eV, corresponding to hopping along the ⟨110⟩ channel and the exchange mechanism along ⟨112⟩ or ⟨001⟩ directions, respectively. We also calculated other two mechanisms which did not occur in experiment, and the barriers are expected to be quite large. When adatom hopping across the bridge site along the ⟨001⟩ direction (the gray circle of Fig. 5(b), the barrier is 2.50 eV, while when hopping over an atop site along the ⟨112⟩ direction [dashed circle of Fig. 5(b)], it is 3.65 eV. The calculated results are again consistent with experiments.[18]

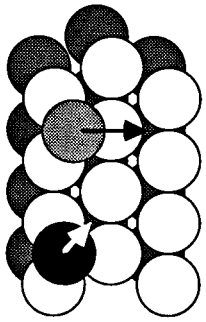

FIG. 4. Single-adatom diffusion by hopping across the bridge site (black circle), and hopping atop the site (gray circle) on the (111) surface.

For the (100) surface, the barrier for the exchange mechanism along the ⟨100⟩ direction (Fig. 7) is 0.79 eV which was

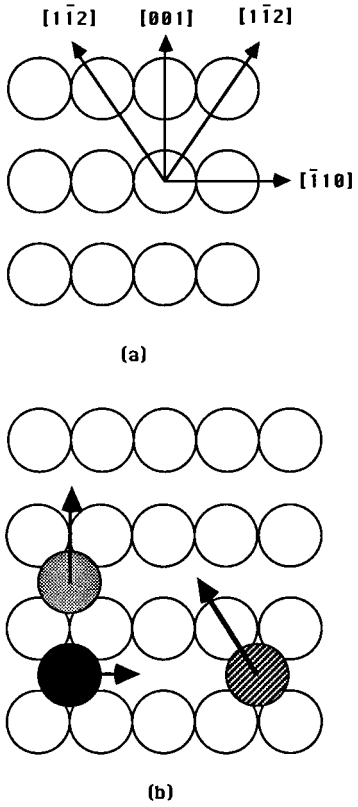

FIG. 5. Along-channel hopping (black circle), cross-channel motion by a hopping bridge site (gray circle), and cross-channel motion by a hopping atop site (dashed circle) of a single adatom on the (110) surface.

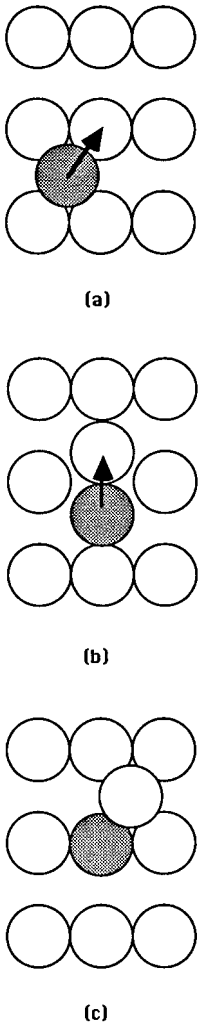

FIG. 6. The cross-channel motion of a single adatom by an exchange mechanism on the (110) face. (a)→(b)→(c) in the ⟨112⟩ direction [and in the ⟨001⟩ direction if the replaced atom move to left instead of right from (b) to (c)].

fitted to experimental results of 0.84 ± 0.05 eV by adjusting the C_{44} shear modulus, as mentioned in Sec. II. The resulting energy barrier for diffusion by hopping over an atop site in the ⟨100⟩ direction [the black circle of Fig. 8(b)] is 2.66 eV. No experimental data exist for this mechanism, but it was believed to be very high.[17] The energy barrier for hopping across the bridge site along the ⟨110⟩ direction [the gray circle of Fig. 8(b)] is 1.58 eV which is smaller than the top site hopping, but still quite large when compared with the exchange mechanism along the ⟨100⟩ direction, and is not observed in experiments.

From these results, we found that the Ir adatom diffuses most easily on the (111) surface ($E_m = 0.11$ eV), less easily on the (110) surface ($E_m = 0.70$ eV), and the least easily on the (100) surface ($E_m = 0.79$ eV). Since the (111) surface is the smoothest and the (100) is the roughest of the three surfaces we studied, a simple rule emerges: *Self-diffusion over atomically smooth surfaces is easier than over rough surfaces*. We also found that there is no exchange mechanism on the (111) surface. This is due to its densely close-packed structure. Because the corrugation of the dense fcc(111) surface is small and does not allow the adatom to penetrate into

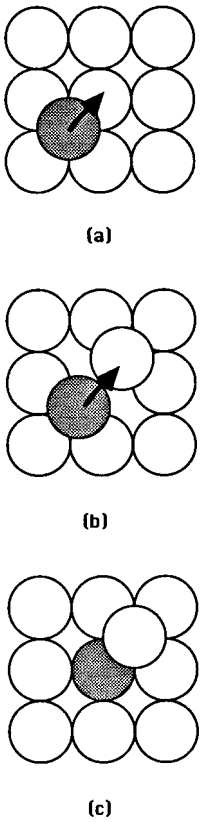

FIG. 7. (a)→(b)→(c) is the path of the exchange mechanism for single-adatom diffusion on a (100) surface.

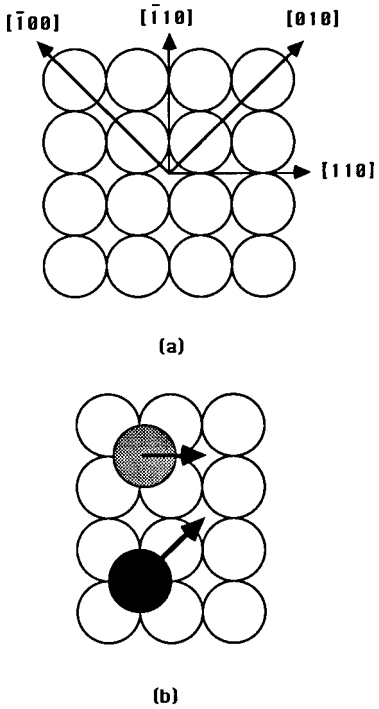

FIG. 8. The diffusion path of a hopping atop site (black circle) and a hopping bridge site (gray circle) for a single adatom on the (100) surface.

TABLE IV. Diffusion path and barriers of Ir_2 dimers on Ir surfaces.

Surface	Diffusion mechanism	Calc. E_m (eV)	Expt. E_m (eV)
(111)	hopping across bridge site with zigzag motion [Fig. 9(a)]	0.17	
	hopping across bridge site with two atoms motion [Fig. 9(b)]	0.30	
	hopping across bridge site with chain reaction [Fig. 9(c)]	0.24	
(110)	hopping along channel with two atoms motion [Fig. 10(a)]	1.25	1.05±0.14 (Ref. 17)
	dissociation and one atom hopping along channel [Fig. 10(b)]	1.31	1.10±0.11 (Ref. 17)
	exchange with chain reaction (Fig. 11)	1.52	1.18±0.12 (Ref. 17)
	exchange wih two atoms motion (Fig. 12)	1.94	
(100)	one atom hopping across bridge site [Fig. 13(a)]	1.63	
	dissociation and one atom hopping across bridge [Fig. 13(b)]	2.65	
	hopping across bridge site with two atoms motion in the perpendicular direction [Fig. 13(c)]	1.69	
	hopping across bridge site with two atoms motion in the parallel direction [Fig. 13(d)]	2.60	
	exchange and dissociation (Fig. 14)	1.52	
	exchange with one atom motion (Fig. 15)	0.65	
	exchange with two atoms motion (Fig. 16)	1.16	

the structure, the adatom can only stay on top of the surface and diffuse over the surface. On the looser (100) surface, there are large and deep spaces that constitute the fourfold surface equilibrium sites for the adatom, and these make the exchange mechanism more likely to occur by a concerted motion where the adatom moves into an adjacent substrate atom and squeezes the substrate atom up to an adjacent fourfold hollow site. For the channeled (110) surface, there are larger space between two adjacent channel walls than the distance between adjacent atoms on the channel wall. Under this condition, the atom on the channel wall can be easily pushed off to an adjacent channel, while the adatom replaces the wall atom to accomplish the exchange mechanism, as observed.[12]

2. Dimers

The diffusion characteristics and energy barriers for Ir_2 dimers on all three Ir surfaces are summarized in Table IV. For the Ir(111) surface, as mentioned in Sec. IV A 2, the energies of dimers on both hcp and fcc sites are almost the same, so the dimers can diffuse between hcp and fcc sites with only a slight difference in the barrier height. Three different mechanisms listed in Table IV and illustrated in Figs. 9(a)–9(c) are the most likely diffusion paths for dimers on the (111) surface. For calculating the zigzag motion as illustrated in Fig. 9(a), we push one adatom by constraining only one coordinate to move across the bridge in the direction perpendicular to the orientation of the dimers to an adjacent site. We found that the ''pushed'' atom will move to the adjacent, different type of site (e.g., from the hcp site to the fcc site) without breaking the bond of the dimer, and form a metastable state. The barrier height in this step is 0.17 eV, which is only slightly higher than the single atom motion of 0.11 eV. The remaining step to finish the diffusion is to drag the other atom of the dimer into the right orientation to form a stable dimer, and the barrier height is a tiny 0.02 eV. Since the barrier for the second step is much smaller, the diffusion time for this step will be very short, and the whole process can be viewed as a one-step process (i.e., once one of the dimer atom jumps to an adjacent site, the other atom will follow spontaneously to form a stable dimer). If we initially push two adatoms to cross the bridge together in the perpendicular direction, as shown in Fig. 9(b), the energy barrier is 0.30 eV. Clearly, this process is not favored. The other case of the chain reaction as illustrated in Fig. 9(c) is by pushing one of the adatoms to move to an adjacent site in the direction diagonal to the dimer orientation, and we found that the other adatom will move with the pushed atom to the adjacent site automatically with a barrier of 0.24 eV. For the unstable state, in which two adatoms sit at different (hcp and fcc)

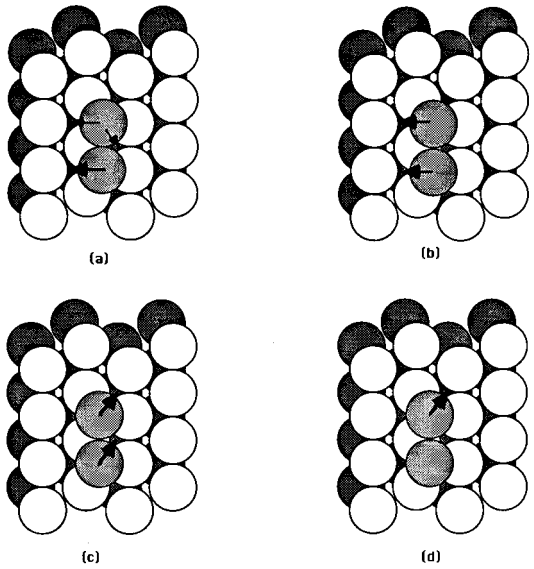

FIG. 9. (a) Dimers diffuse with a zigzag motion on the (111) surface. The large arrow suggests the first jump, the small arrow the second. There are two possible directions for the second jump: a jump to the left to complete the local translation, or a jump to the lower right to complete the rotational motion. (b) Local translation. (c) Intercell translation. (d) Forbidden path for dimer diffusion on the (111) plane.

types of sites at the second-nearest-neighbor spacing, diffusion by dissociation and coupled with a single adatom jump to the adjacent site, as depicted in Fig. 9(d), is not possible because of the high-energy barrier (see Sec. IV A 2). Therefore, if one of the dimer atoms jumps to the adjacent site in the diagonal direction, the other atom must be dragged along. From these results we found that the local translation is likely to be accomplished by a zigzag motion [Fig. 9(a)] which can be also accomplished by two local 30° rotations. The intercell translation is accomplished by the chain reaction [Fig. 9(c)].

For the (110) surface, we calculated four possible diffusion mechanisms illustrated in Figs. 10–12. Figure 10(a) shows the mechanism of hopping along the surface ⟨110⟩ channel by two-atom motion, and the energy barrier is 1.25 eV, which is comparable to the FIM result of 1.05 eV.[17] The calculated result of 1.25 eV is larger than the single-adatom hopping of 0.70 eV, but is smaller than twice the barrier energy of 1.40 eV. This reduction of energy is due to the attractive interactions between two Ir adatoms. The Ir_2 dimer presumably can dissociate into two individual atoms and diffuse as a single adatom, as shown in Fig. 10(b). The barrier height for this process is 1.31 eV, which is higher than the two-atom motion [Fig. 10(a)], and is about the value of the single-adatom hopping of 0.70 eV plus the binding energy of 0.64 eV (Table II). The experimental value for this mechanism is 1.10 eV. Figure 11 illustrates the exchange mechanism of Ir_2 dimers, and the process is done by successive one-atom and correlated jumps. The diffusion barrier for this chain reaction is 1.52 eV. The experimental value for this process is 1.18 eV. For the case of exchange with two-atom motion as illustrated in Fig. 12, the energy barrier is 1.94 eV. From these results, we therefore believe that Ir_2 dimers on the Ir(110) surface tend to diffuse along the surface channel

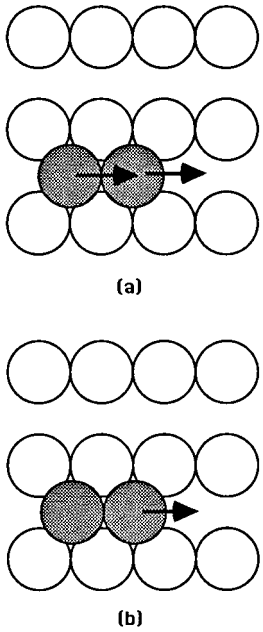

FIG. 10. The diffusion path of dimers on the (110) surface (a) by hopping along a channel with two-atom motion, and (b) by dissociation and one-atom (indicated by arrow) hopping along a channel.

with a concerted motion as shown in Fig. 10(a).

For the (100) surface we calculated seven possible processes, four with the hopping across the bridge site, and three with exchange mechanisms (Figs. 13–16). Figure 13(a) shows one-adatom hopping across the bridge site in a direction perpendicular to the dimer orientation, and the barrier height is 1.63 eV, which is about the value of a single-adatom hopping across the bridge site (1.58 eV). It seems that in this mechanism the interaction between two adatoms has a very small influence on the barrier energy in the diffusion process, and causes the jump in the same way as single-adatom diffusion. Shown in Fig. 13(b) is the process by which a dimer is dissociated, and one atom jumps across the bridge site in a direction parallel to the orientation of the

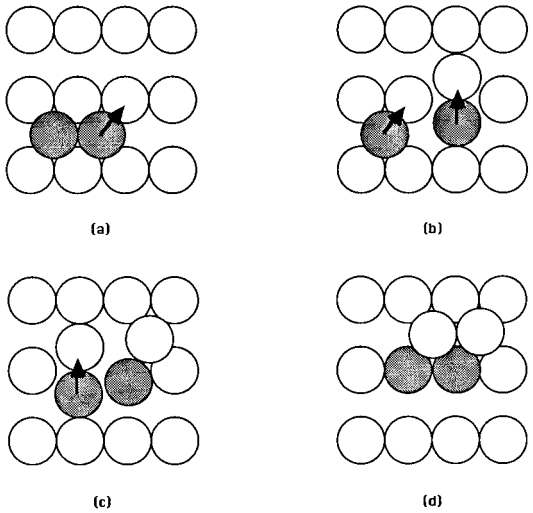

FIG. 11. The chain reaction path of exchange mechanism for dimers on the (110) surface. (a)→(b)→(c)→(d).

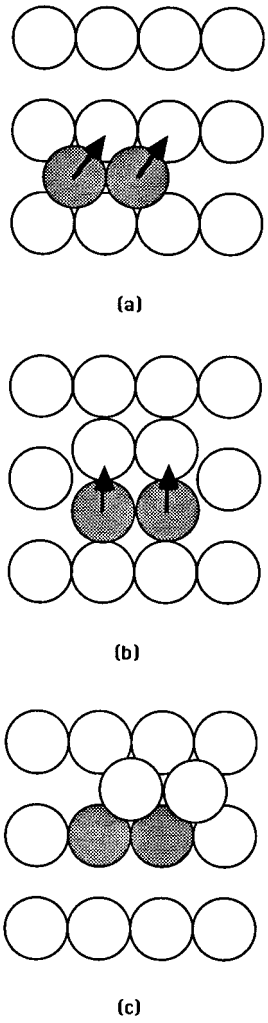

FIG. 12. The path of two atoms moving together by an exchange mechanism on the (110) surface. (a)→(b)→(c).

dimer. The activation energy for this process is 2.65 eV. This high value is just a little bit higher than the value of single-adatom hopping, 1.58 eV, plus the binding energy of 0.79 eV. For two adatom hopping across bridge sites together in a perpendicular direction, as illustrated in Fig. 13(c), the diffusion energy is 1.69 eV, which is significantly lower than twice the energy of single-adatom hopping. If the cross-bridge hopping of the two-atom motion is in the parallel direction, as indicated in Fig. 13(d), the barrier height is 2.60 eV. Figure 14 shows the dissociation and exchange mechanism with a barrier height of 1.52 eV, which is roughly the sum of the binding energy (0.79 eV) and the energy of single-adatom exchange (0.79 eV). *The mechanism of exchange without dissociation, as shown in Fig. 15, has an interestingly low-energy barrier of 0.65 eV, which is even lower than the barrier of a single-adatom exchange.* This is not unreasonable since, in the exchange process, the two adatoms and the surface atom which is to be substituted remain at close attractive interaction distances and reduce the barrier height. Figure 16 shows the exchange mechanism with the two-atom motion, with a barrier height of 1.16 eV, which is also higher than the single-adatom exchange and lower than twice the single-adatom exchange barrier. Unfortunately, no experimental results exist for Ir_2 dimer diffusion on the

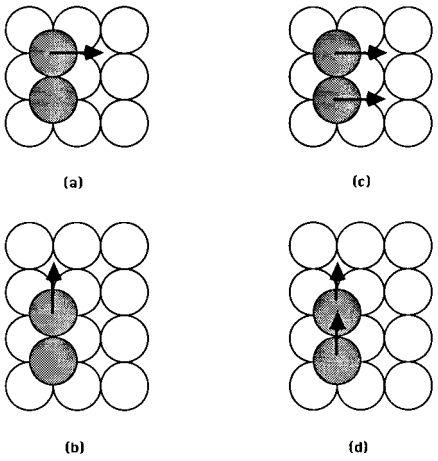

FIG. 13. Diffusion path of dimers on the (100) surface. (a) One-atom (indicated by arrow) hopping bridge to the second-nearest neighbor. (b) Dissociation and one-atom (indicated by arrow) hopping bridge to the third-nearest neighbor. (c) Hopping bridge, where two atoms move together in a direction perpendicular to the orientation of the dimers. (d) Hopping bridge, where two atoms move together in a direction parallel to the orientation of the dimers.

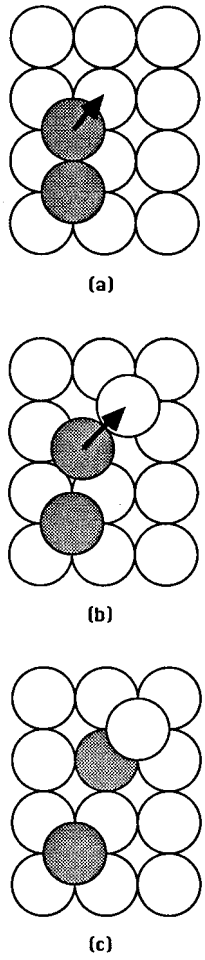

FIG. 14. The path of dimer diffusion (a)→(b)→(c) by dissociation and one-atom (indicated by arrow) exchange, with the surface atom on the (100) surface.

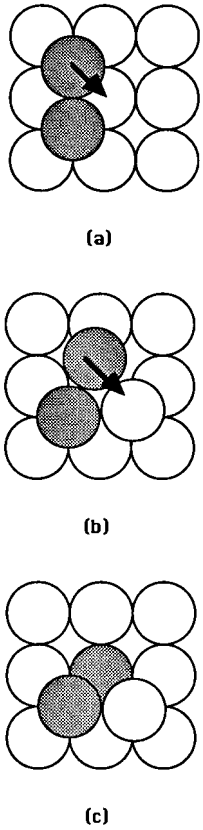

FIG. 15. The most favorable path of dimer diffusion on the (100) surface (a)→(b)→(c) by one-atom exchange with the surface atom, and a rotation of the orientation of the dimers.

Ir(100) surface. It will be very interesting for experimentalists to check out whether the low diffusion barrier predicted here for Ir_2 dimers on the Ir(100) surface actually occurs.

3. N-mers (N≥3)

In this subsection, we focus our attention on the diffusional behavior of small Ir clusters (trimers, tetramers, and pentamers) on the Ir(111) surface (Table V and Figs. 17–21). Since the most stable structure on the (111) surface for small clusters is the two-dimensional close-packed structures, we only studied the diffusion of three clusters with 2D structures. For the diffusion of Ir trimers, we found that the trimer tends to diffuse together. There are two possible paths which still retain a triangular form after diffusion, as indicated in Figs. 17(a) and 17(b) (Table V). The energy barriers for these two diffusion mechanisms are 0.56 and 0.54 eV, respectively, and are in good agreement with FIM results of 0.63 eV.[15] The mechanism shown in Fig. 17(a) has a higher barrier than that of Fig. 17(b). The reason for this is that atom 1 in Fig. 17(a) has to drag atoms 2 and 3 at the same time for the trimer to move, while for the mechanism shown in Fig. 17(b) there are no such difficulties. The trimer diffuses in the following sequence: atom 1 drags atom 2, then atom 2 pushes atom 3 and forces all three atoms to move together. In other words, atoms 2 and 3 in Fig. 17(a) diffuse as in the case of local translation, with a two-atom motion for the dimer and thus a higher barrier. The long-range intercell translations for trimers are achieved by successive diffusions in Figs. 17(a) and 17(b).

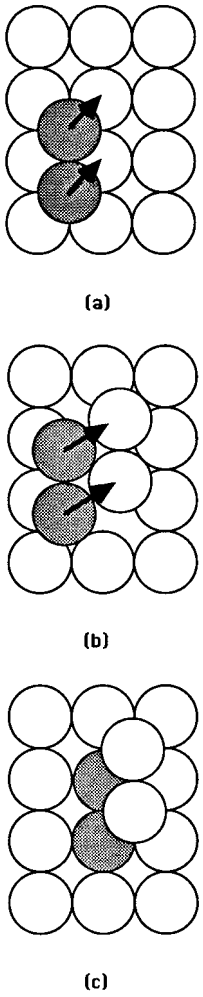

FIG. 16. Dimer diffusion path on the (100) face by two-atom exchange with surface atoms together. (a)→(b)→(c).

The tetramer also tends to diffuse together in our simulations. We found that once we push one of the tetramer atoms the whole cluster will move together. The most favorable diffusion path for tetramers is illustrated in Fig. 18 with a barrier of 0.54 eV, which is surprisingly low and in reasonable agreement with experimental data of 0.46 eV.[15] We do not find any rotational mechanisms for tetramers and trimers on the (111) surface.

TABLE V. Diffusion path and barriers of small Ir clusters on an Ir(111) surface.

Number of adatoms	Diffusion mechanism	Calculated E_m (eV)	Experimental E_m (eV) (Ref. 15)
Single adatom	hopping bridge	0.11	0.27±0.004
			0.22±0.04 (Ref.17)
Dimer	rotation	0.17	0.43±0.013
	translation	0.24	
Trimer	translation	0.54	0.63±0.017
		0.56	
Tetramer	translation	0.54	0.46±0.013
Pentamer	rotation	0.83	0.66±0.013
	translation	0.92	
		1.18	

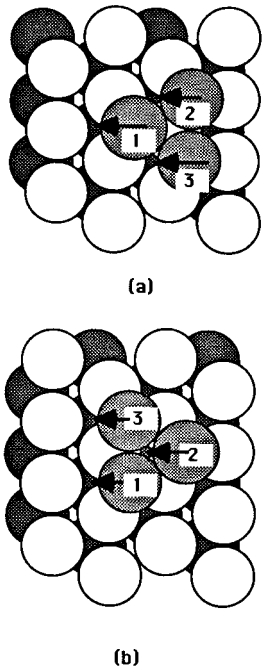

FIG. 17. Diffusion path for trimers on the (111) surface. (a) Atom 1 drags atoms 2 and 3, and then the three atoms move together. (b) Atom 1 drags atom 2, then atom 2 pushes atom 3, and the three atoms move together.

For pentamers, we found that the rotation mechanism, as indicated in Fig. 19, is the most favorable diffusion path. The diffusion barrier for this rotational motion is 0.83 eV, while for the translational motions shown in Figs. 20(a) and 20(b) the barriers are 0.92 and 1.18 eV, respectively. For the mechanism shown in Fig. 20(a), we only push atom 1, and the rest of the clusters follow the lead atom (atom 1) automatically. In Fig. 20(b), we force atoms 1 and 2 to move together, and then the other three adatoms will move with the two lead atoms (atoms 1 and 2).

From the results shown in Table V and Fig. 21, we indeed found the qualitative trend that has been observed in FIM experiments:[14,15] the migration energy increases sharply from adatom to dimers, and from dimers to trimers, then drops for tetramers, and then rises again for pentamers. Even though the qualitative trends of E_m as a function of N is the same as in the experiment, the diffusion mechanisms derived from our collective motion of atoms are different from the single-atom jumps proposed in Ref. 15.

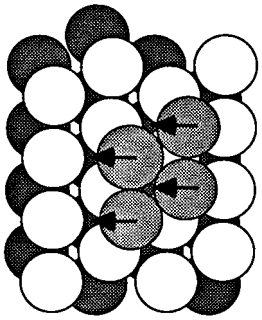

FIG. 18. The most favorable diffusion path for tetramers on the (111) surface.

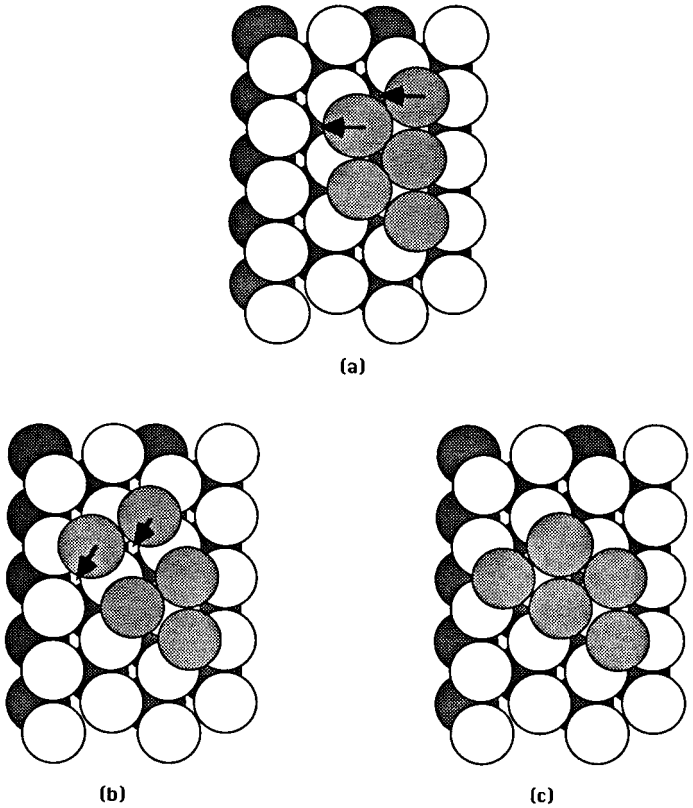

FIG. 19. Rotation of pentamers on the (111) surface (a)→(b)→(c).

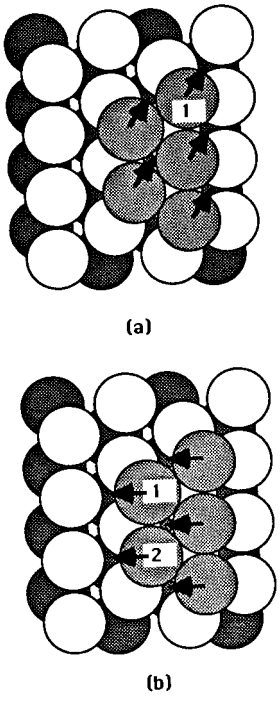

FIG. 20. Translation path of pentamers on the (111) surface. (a) Push atom 1 and others will move with it. (b) Push atoms 1 and 2, and then the others will move together.

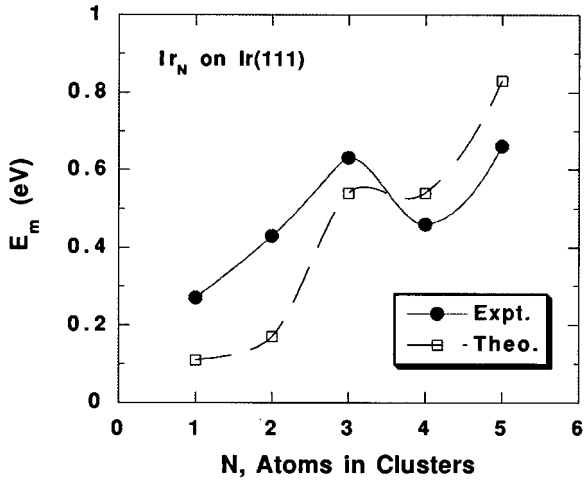

FIG. 21. The theoretical and experimental (Ref. 17) migration energies of Ir N-mers, Ir_N, on the Ir(111) surface.

V. CONCLUSIONS

As already mentioned, cluster structure and surface diffusion plays an important role in understanding many surface phenomena. The goal of this paper is to study how small iridium clusters adsorb and migrate on various iridium surfaces using EAM potentials. For single-adatom diffusion, the mobility is much higher on the (111) surface than on the rougher (100) and (110) surfaces, because the migration energies increase with the surface roughness. The exchange mechanism on the (100) surface is indeed favored over the hopping mechanism, while, for the (110) surface, both atomic motions along and across the atomic channel are possible because these two mechanisms have similar activation energies (0.70 vs 0.81 eV). For two adatoms, the Ir_2 dimer with the nearest-neighbor spacing is the most stable structure on all three faces. The dimer retains[9] 1D structure on a (100) surface, and (110), and a 2D structure on a (111) surface. Dimers tend to diffuse in concerted motion instead of individual atom motion on (110) and (111) surfaces, while individual atomic exchange is favored on the (100) surface. Ir dimer favors hopping along the channel on the (110) surface, while for the (111) surface an interesting zigzag swaying motion on fcc and hcp sites is favored. The anomalous low activation energy for a dimer on the (100) plane indicates that the migration energy does not always increase from the adatom to the dimer, but this should be checked by experiments. For small clusters that can have either 1D or 2D configurations, we found that, on the looser (100) and (110) faces, the adatoms tend to line along the packed atomic row, while on the dense (111) surface they tend to form a close-packed 2D structure. The small clusters on the (111) surface tend to translate together, but, for larger clusters, pentamers for example, the rotation mechanism is more favorable. The unusual and interesting activation energy drops (or stays flat) from trimers to tetramers is indeed confirmed by our calculations.

ACKNOWLEDGMENTS

We would like to acknowledge the U.S. Department of Energy and the National Science Council of R.O.C. (under Grant No. NSC84-2112-M-001-006) and Academia Sinica for financial support. S.P.C. would also like to thank the NSC of R.O.C. for its support for his summer visit at the Institute of Physics, Academia Sinica in 1992. We would also like to thank T. T. Tsong for helpful discussions.

[1] A. Zangwill, *Physics at Surfaces* (Cambridge University Press, Cambridge, 1988).
[2] E. W. Müller and T. T. Tsong, *Field Ion Microscopy, Principles and Applications* (Elsevier, New York, 1969).
[3] G. Ayrault and G. Ehrlich, J. Chem. Phys. **60**, 281 (1974).
[4] P. F. Feibelman, J. S. Nelson, and G. L. Kellogg, Phys. Rev. B **49**, 10 548 (1994).
[5] D. W. Bassett and P. R. Webber, Surf. Sci. **70**, 520 (1978).
[6] R. T. Tung and W. R. Graham, Surf. Sci. **97**, 73 (1980).
[7] G. Ehrlich and F. G. Hudda, J. Chem. Phys. **44**, 1039 (1966).
[8] P. L. Cowan and T. T. Tsong, Phys. Lett. A **53**, 383 (1975).
[9] T. T. Tsong, P. L. Cowan, and G. L. Kellogg, Thin Solid Films **25**, 97 (1975).
[10] W. R. Graham and G. Ehrlich, Surf. Sci. **45**, 530 (1974).
[11] D. W. Bassett and M. J. Parsley, J. Phys. D **2**, 13 (1969); D. W. Bassett and P. R. Webber, J. Phys. C **9**, 2491 (1976).
[12] J. D. Wrigley and G. Ehrlich, Phys. Rev. Lett. **44**, 661 (1980); C. L. Chen and T. T. Tsong, Appl. Phys. A **51**, 405 (1990); G. Ehrlich, Surf. Sci. **299/300**, 628 (1994).
[13] S. C. Wang and G. Ehrlich, Surf. Sci. **246**, 37 (1991).
[14] G. Ehrlich, Surf. Sci. **246**, 1 (1991).
[15] S. C. Wang and G. Ehrlich, Surf. Sci. **239**, 301 (1990).
[16] C. L. Chen and T. T. Tsong, Phys. Rev. B **41**, 12 403 (1990).
[17] C. L. Chen and T. T. Tsong, Phys. Rev. Lett. **64**, 3147 (1990); T. T. Tsong, in *Surface Physics*, edited by X. Li, Z. Qin, D. Shen, and D. Wang (Gordon and Breach, Philadelphia, 1992), p. 75.
[18] T. T. Tsong and C. L. Chen, Phys. Rev. B **43**, 2007 (1991).
[19] C. L. Chen and T. T. Tsong, Phys. Rev. Lett. **66**, 1610 (1991).
[20] T. T. Tsong and C. L. Chen, Surf. Sci. **246**, 13 (1991).
[21] P. R. Schwoebel and G. L. Kellogg, Phys. Rev. B **38**, 5326 (1988).
[22] V. R. Dhanak and D. W. Bassett, Surf. Sci. **238**, 289 (1990).
[23] R. T. Tung, Ph.D. thesis, University of Pennsylvania, 1980 (unpublished).
[24] J. C. Tully, G. H. Gilmer, and M. Shugard, J. Chem. Phys. **71**, 1630 (1979).
[25] C. L. Liu, J. M. Cohen, J. B. Adams, and A. F. Voter, Surf. Sci. **253**, 334 (1991).
[26] H. K. McDowell and J. D. Doll, J. Chem. Phys. **78**, 3219 (1983).
[27] J. D. Doll and H. K. McDowell, J. Chem. Phys. **77**, 479 (1982).
[28] S. C. Park and J. M. Bowman, J. Chem. Phys. **80**, 2191 (1984).
[29] P. J. Feibelman, Phys. Rev. Lett. **65**, 729 (1990).
[30] G. L. Kellogg and P. J. Feibelman, Phys. Rev. Lett. **64**, 3143 (1990).
[31] R. M. Lynden-Bell, Surf. Sci. **259**, 129 (1991).
[32] S. M. Foiles, Phys. Rev. B **32**, 3409 (1985); T. L. Einstein, in

Physical Structure of Solid Surfaces, edited by W. N. Unertl (Elsevier/North-Holland, Amsterdam, 1995), Chap. 11.
[33] J. B. Adams, S. M. Foiles, and W. G. Wolfer, J. Mater. Res. **4**, 102 (1989).
[34] C. L. Liu and J. B. Adams, Surf. Sci. **265**, 262 (1992).
[35] J. C. Hamilton, M. S. Daw, and S. M. Foiles, Phys. Rev. Lett. **74**, 2760 (1995).
[36] Wei Xu and J. B. Adams, Surf. Sci. **301**, 371 (1994); **319**, 45 (1994); **319**, 58 (1994); G. H. Campbell, S. M. Foiles, P. Gumbsch, M. Rühle, and W. E. King, Phys. Rev. Lett. **70**, 449 (1993).
[37] T. L. Einstein, M. S. Daw, and S. M. Foiles, Surf. Sci. **227**, 114 (1990).
[38] T. L. Einstein, Langmuir **7**, 2520 (1991).
[39] W. D. Wilson, Phys. Rev. B **24**, 5616 (1981).
[40] M. S. Daw and M. I. Baskes, Phys. Rev. B **29**, 6443 (1984).
[41] M. S. Daw and M. I. Baskes, Phys. Rev. Lett. **50**, 1285 (1983).
[42] M. S. Daw and R. D. Hatcher, Solid State Commun. **56**, 697 (1985).
[43] S. M. Foiles, M. I. Baskes, and M. S. Daw, Phys. Rev. B **33**, 7983 (1986).
[44] A. F. Voter and S. P. Chen, in *Characterization of Defects in Materials*, edited by R. W. Siegel, R. Sinclair, and J. R. Weertman, MRS Symposia Proceedings No. 82 (Materials Research Society, Pittsburgh, 1987), p. 175.
[45] S. P. Chen, D. J. Srolovitz, and A. F. Voter, J. Mater. Res. **4**, 62 (1989).
[46] S. P. Chen, A. F. Voter, R. C. Albers, A. M. Boring, and P. J. Hay, J. Mater. Res. **5**, 955 (1990).
[47] S. P. Chen, A. F. Voter, and D. J. Srolovitz, Phys. Rev. Lett. **57**, 1308 (1986).
[48] S. P. Chen, Philos. Mag. A **66**, 1 (1992).
[49] S. P. Chen, Surf. Sci. Lett. **274**, L619 (1992).
[50] S. P. Chen, Surf. Sci. Lett. **264**, L162 (1992).
[51] M. Karimi and Mark Mostoller, Phys. Rev. B **45**, 6289 (1992).
[52] J. S. Nelson, Erik C. Sowa, and M. S. Daw, Phys. Rev. Lett. **61**, 1977 (1988).
[53] J. S. Nelson, M. S. Daw, and Erik C. Sowa, Phys. Rev. B **40**, 1465 (1989).
[54] Liqiu Yang, Talat S. Rahman, and M. S. Daw, Phys. Rev. B **44**, 13 725 (1991).
[55] W. K. Rilling, C. M. Gilmore, T. D. Andreadis, and J. A. Sprague, Can. J. Phys. **68**, 1035 (1990).
[56] Z. J. Tian and T. S. Rahman, Phys. Rev. B **47**, 9751 (1993).
[57] R. C. Nelson, T. L. Einstein, S. V. Khare, and P. J. Rous, Surf. Sci. **295**, 462 (1993).
[58] L. D. Roelofs and E. I. Martir, in *The Structure of Surfaces III*, edited by S. Y. Tong, M. A. Van Hove, K. Takayanagi, and X. D. Xie (Springer, Berlin, 1991), p. 248.
[59] P. A. Gravil and S. Holloway, Surf. Sci. **310**, 267 (1994).
[60] J. H. Rose, J. R. Smith, F. Guinea, and J. Ferrante, Phys. Rev. B **29**, 2963 (1984).
[61] P. Flynn, *Point Defects and Diffusions* (Clarendon, Oxford, 1972), Chap. 7.
[62] S. P. Chen and A. F. Voter, Surf. Sci. Lett. **244**, L107 (1991).